Accelerating Membrane Insertion of Peripheral Proteins with a Novel Membrane Mimetic Model

Y. Zenmei Ohkubo, Taras V. Pogorelov, Mark J. Arcario, Geoff A. Christensen, and Emad Tajkhorshid

Beckman Institute for Advanced Science and Technology, Department of Biochemistry, Center for Biophysics and Computational Biology, College of Medicine, School of Chemical Sciences, University of Illinois at Urbana-Champaign, Urbana, Illinois

Supporting Information

Materials and methods in detail

In this section, after describing the HMMM model, we provide the details of the various simulations performed to (1) describe spontaneous formation of a bilayer-like structure by the model, (2) quantify the lipid mobility of the model and the effects of simulation conditions and configurations on the mobility, and (3) capture in repeated simulations spontaneous binding and insertion of a prototype membrane-anchoring domain, the GLA domain of human coagulation factor VII (hFVII), to the surface of anionic membranes.

General aspects of the HMMM model

The design of the HMMM model is based on a conceptually simple, but novel idea of replacing the hydrophobic core of a lipid bilayer, where interactions with proteins and other membrane-interacting molecules are usually non-specific van der Waals interactions and the long acyl tails cause significant friction against lateral diffusion of lipids, with a more fluid apolar organic solvent in order to introduce enhanced mobility. The organic phase is sandwiched by two layers of water representing the aqueous solution on either side of the membrane core. Short-tailed lipids (st-lipids), which are generated by shortening the length of the acyl chains while preserving the full atomic details of the headgroups, are then used to line the interfacial regions between the organic and aqueous phases. In the HMMM membrane used in the present study, 1,1-dichloroethane (DCLE) is used to model the hydrophobic core of the bilayer, and divalerylphosphatidylserine (DVPS) molecules to represent the phosphatidylserine (PS) lipids, which are known to be necessary for binding of the coagulation proteins, thus pertinent to the studied membrane-anchoring domain here. The organic phase was chosen such that the organic molecule was relatively small, had a low aqueous solubility in order to maintain a biphasic solvent system, remained a liquid at physiological temperature, and had readily available parameters (45). DCLE was determined to be the optimum choice of solvent based on these constraints. For instance, DCLE has eight atoms (only four of which are heavy atoms), an aqueous solubility of 8.6×10^{-3} g/mL H_2O, a boiling point of 330 K (78), and the parameters for this molecule are available in the CHARMM36 General Force Field (51).

The HMMM model can be readily constructed with other st-lipids, *e.g.*, phosphatidic acid (PA), phosphatidylcholine (PC), phosphatidylethanolamine (PE), and phosphatidylglycerol (PG), as well as mixtures of these headgroups. Thus, the chemical composition of the bilayer can be easily tuned to the specific applications of the model. The thickness of the hydrophobic core, and thereby the membrane, can also be readily adjusted in the HMMM model by simply adjusting the volume of the organic phase. In our system, the biphasic solvent box and the lipids were prepared separately and then combined by aligning their respective centers of masses (COMs) to the origin of the final simulation system. The water and DCLE molecules that overlapped with DVPS lipids (within 1.2 Å and 0.9 Å, respectively) were removed, and counterions (Ca^{2+} or Na^{+}) were added to neutralize the system.

The topology for DCLE was adopted from CHARMM36 (51), and DCLE coordinates were generated as described elsewhere (45). The topology for DVPS st-lipids (the number of carbons in the acyl tail, n, is 5) was generated from that of 3-palmitoyl-2-oleoyl-D-glycero-1-phosphatidylserine (POPS, $n = 18$) in CHARMM36 (51) by shortening both tails of POPS, *i.e.*, removing C25–C217, C35–C315, and associated hydrogen atoms and forming single bonds between C24 and C218 and between C34 and C316 (45). The topology for DVPS is provided as a separate supplementary file available for download by the interested users. Since no new atom type was needed, the provided topology file will work with the standard distribution of CHARMM36 (51). Table 1 summarizes all the simulation systems described in the present study including different configurations of the HMMM model and two full membrane simulations used as references to compare the properties of the two membrane representations; the dimensions of the unit cell and DVPS grid points for these HMMM systems are shown in Table S1. These simulations are described below in detail.

Spontaneous formation of the HMMM membrane

To investigate the efficiency and robustness of the HMMM model, its ability to form and maintain bilayers was tested in a simulation in which the st-lipids were initially distributed on a grid spanning the whole volume of the biphasic solvent box, with approximately half of the molecules in the organic phase and the other half in water. A DCLE/water biphasic box of $60 \times 60 \times 120$ Å^3 ($x \times y \times z$), prepared elsewhere (45), was used for the simulation of the membrane formation. The box consisted of a 60-Å-thick DCLE layer representing the acyl tail region, sandwiched by two 30-Å-thick water layers. A pre-equilibrated (5 ps) DVPS

molecule was replicated in space on a grid overlapping the biphasic solvent system in order to generate the initial arrangement of the lipids. The set of replicated lipids included 54 DVPS lipids placed on a 3×3×6 (along the x, y, and z axis) grid with the same edge length (20 Å). The orientations of the individual lipids were randomized (Fig. 2, top left panel).

Examining the effect of density on lipid mobility

Another set of five simulations were performed to calculate the lateral diffusion constant of the lipids in the HMMM model and its dependence on different configurations, including lipid density and the type of counterion used. These systems were constructed to include a larger patch of a pre-formed HMMM membrane (120×120 Å^2) composed of 49, 100, 144 (in the presence of Na^+ or Ca^{2+} counterions), and 210 DVPS lipid molecules per leaflet, respectively, corresponding to the area per lipid, A_L, of 294.0, 144.0, 100.0, and 68.6 Å^2 (Table 1). The DVPS molecules were initially placed along the two interfacial planes of the biphasic solvent system with the PS headgroups protruding into the water layers. The orientation of individual lipids was then randomized fully about the z axis (the membrane normal) and within ±10 degrees along the x and y axes. All of these simulation systems included a 35-Å-thick DCLE layer sandwiched by two 20-Å-thick water layers (Supporting Information).

The lateral (two-dimensional) diffusion constant, D, of lipids was obtained as the asymptote of the ensemble average of the mean-square displacement of the atoms of interest, $D(t)$,

$$D = \lim_{t\to\infty} D(t) = \frac{1}{2d} \lim_{t\to\infty} \frac{\langle |r(t_0 + t) - r(t_0)|^2 \rangle}{t} \tag{S1}$$

where $r(t_0)$ is the position of a lipid (represented by the phosphorus atom in this study) at time t_0, $r(t_0 + t)$ is the position of the lipid after a time lag of t, and d is the dimension (= 2 for the two-dimensional lateral diffusion constant; with the z component of r excluded from the computation) (45, 76). The computed $D(t)$ for the HMMM membranes converges quickly with t and reached the asymptotic value at around $t = 5$ ns in our simulations. As such, we selected the last 10 ns of individual simulations from which D was obtained as the average of $D(t)$.

Insertion of the GLA domain into the HMMM model

Ten independent simulations were performed to test the efficiency of the HMMM model in

capturing membrane binding of a membrane anchor in unbiased simulations. The system used for these simulations included a pre-formed HMMM membrane composed of a biphasic solvent box of $90\times90\times100\,\text{Å}^3$ and 128 DVPS lipids initially placed on two 8×8 2D grids along the two interfacial planes between water and DCLE layers. The GLA domain of hFVII with seven bound Ca^{2+} ions was based on PDB ID: 1DAN (48), which has been equilibrated in solution elsewhere (49). In each membrane binding simulation, the GLA domain was positioned in the bulk water at least 8 Å above the DVPS surface with its membrane-anchoring ω-loop (49) pointing towards the membrane (Fig. 5, left inset). After removing overlapping water and DCLE molecules (within 1.2 Å of the GLA domain), the system was neutralized by randomly replacing water molecules with Na^+ ions. The system was then subjected to energy minimization and a short equilibration with weak harmonic constraints on Cα atoms of the GLA domain and phosphorus atoms of DVPS before it was fully equilibrated without constraints for 50 ns. This simulation was repeated 10 times.

Full membrane simulations

As a reference, a full membrane composed of 288 DOPS (1,2-dioleoyl-*sn*-glycero-3-phospho-L-serine) molecules was also simulated with either Na^+ or Ca^{2+} as the counterion (we refer to these conventional membrane models as "full membranes" to contrast them with the HMMM model). The size of the membrane patch was $97\times97\,\text{Å}^2$, chosen to correspond to the experimentally estimated A_L for this lipid ($65.3\,\text{Å}^2$; (77)). The system was simulated for 20 ns as an NP_nAT (P_n for constant membrane-normal pressure and A for the membrane area) ensemble and using the conditions described elsewhere (47).

Simulation protocols

All the simulations were performed using NAMD2 (50) with the CHARMM36 force field parameter set (51), the CMAP corrections (52) for proteins, and the TIP3P model for water (53) in the NP_nAT ensemble. Langevin dynamics with a damping coefficient, γ, of $0.5\,\text{ps}^{-1}$ and Langevin piston Nosé-Hoover methods (54, 55) were employed to maintain the temperature at 310 K and pressure at 1 atm, respectively. To evaluate long-range electrostatic forces without truncation, the particle mesh Ewald (PME) method (56) with a grid density of slightly finer than $1\,\text{Å}^{-3}$ was used. The cut-off for van der Waals interaction was set at 12 Å. Integration time steps were set at 2, 2, and 4 fs for bonded, nonbonded, and PME

calculations, respectively. For the simulations of full DOPS membranes integration time steps of 1, 1, and 2 fs (for bonded, nonbonded, and PME) and CHARMM27 force field parameters were used; other conditions were the same as the above.

Table S1: **System configurations**. The systems simulated in this study for spontaneous membrane formation (HMMM-0), diffusion constant calculation (HMMM-1 to HMMM-5, Full-1, Full-2), and GLA domain binding (HMMM-GLA) are listed along with the membrane-forming lipid, the number of the acyl tail carbons (n), the dimensions of the unit cell and DVPS grid points, the counterion, the area per lipid (A_L), as well as the measured lateral diffusion constant of the lipids (D). $*$, distance between phosphorus atom layers; n.a., not applicable; –, not measured. Simulation of System HMMM-GLA was repeated 10 times.

System	Lipid	n	Membrane size / Å^2 $x\times y$	Layer thickness / Å $+z$ H_2O/DCLE/-z H_2O	Grid points $x\times y\times z$	Grid point gaps / Å $x\times y\times z$	Counterion	A_L / Å^2	D / 10^{-8} cm^2 s^{-1}
HMMM Simulations									
HMMM-0	DVPS	5	60× 60	30 / 60 / 30	3× 3×6	20.0×20.0×20.0	Na^+	133.0	–
HMMM-1	DVPS	5	120×120	20 / 35 / 20	7× 7×2	15.0×15.0×35.0	Na^+	294.0	314.0
HMMM-2	DVPS	5	120×120	20 / 35 / 20	10×10×2	11.0×11.0×35.0	Na^+	144.0	171.0
HMMM-3	DVPS	5	120×120	20 / 35 / 20	10×10×2	11.0×11.0×35.0	Ca^{2+}	144.0	134.0
HMMM-4	DVPS	5	120×120	20 / 35 / 20	12×12×2	9.2× 9.2×35.0	Na^+	100.0	97.7
HMMM-5	DVPS	5	120×120	20 / 35 / 20	14×15×2	8.0× 7.5×35.0	Na^+	68.6	26.4
GLA Domain Binding									
HMMM-GLA (×10)	DVPS	5	90× 90	50 / 30 / 20	8× 8×2	10.7×10.7×30.0	Na^+	127.0	–
Full Membrane Simulations									
Full-1	DOPS	18	97× 97	22 / 39*(DOPS) / 22	n.a.	n.a.	Na^+	65.3	4.93
Full-2	DOPS	18	97× 97	22 / 39*(DOPS) / 22	n.a.	n.a.	Ca^{2+}	65.3	2.10

Repeated simulations of spontaneous membrane binding of the GLA domain

Figure S1. Spontaneous bindings of the GLA domain to the HMMM membranes. MD simulation of membrane binding of the GLA domain to the HMMM DVPS membrane (Fig. 5) was repeated 10 times. The GLA domain established initial contacts with the membrane in as quickly as 2 ns (**A**) and 4 ns (**B**), although in some cases the protein spent a long time diffusing in bulk water before approaching the membrane (**C**).

The data are presented using the same schemes for Figs. 5 and 6:
The top panel shows the average heights of the GLA-bound Ca^{2+} ions (red line), the Cα atoms of residues 4–8 in the ω-loop (blue), the carboxy carbon atoms of DVPS lipids (black), the phosphate phosphorus atoms of DVPS lipids (black), and the C_5 atoms of DVPS acyl tails (black) as a function of simulation time.

The bottom panel depicts time series for specific interactions between the GLA domain and the DVPS lipids in terms of the number of the contribution of various moieties of the lipid head groups: *(first row)* the number of phosphate phosphorus atoms within 5.0 Å of any basic side chains of the GLA domain (black bars); *(second row)* the number carboxy carbon atoms within 5.0 Å of any basic side chains of the GLA domain (red); *(third row)* the number of phosphate phosphorus atoms within 5.0 Å of any GLA-bound Ca^{2+} ions (green); and *(fourth row)* the number of carboxy carbon atoms within 5.0 Å of any GLA-bound Ca^{2+} ions (blue).

The average numbers of either phosphate or carboxy groups that are within 5.0 Å, with the standard deviation below in parentheses, are obtained from the t = 30–50 ns portion of the MD simulation. Matching colors are used for the same interactions shown in different panels.

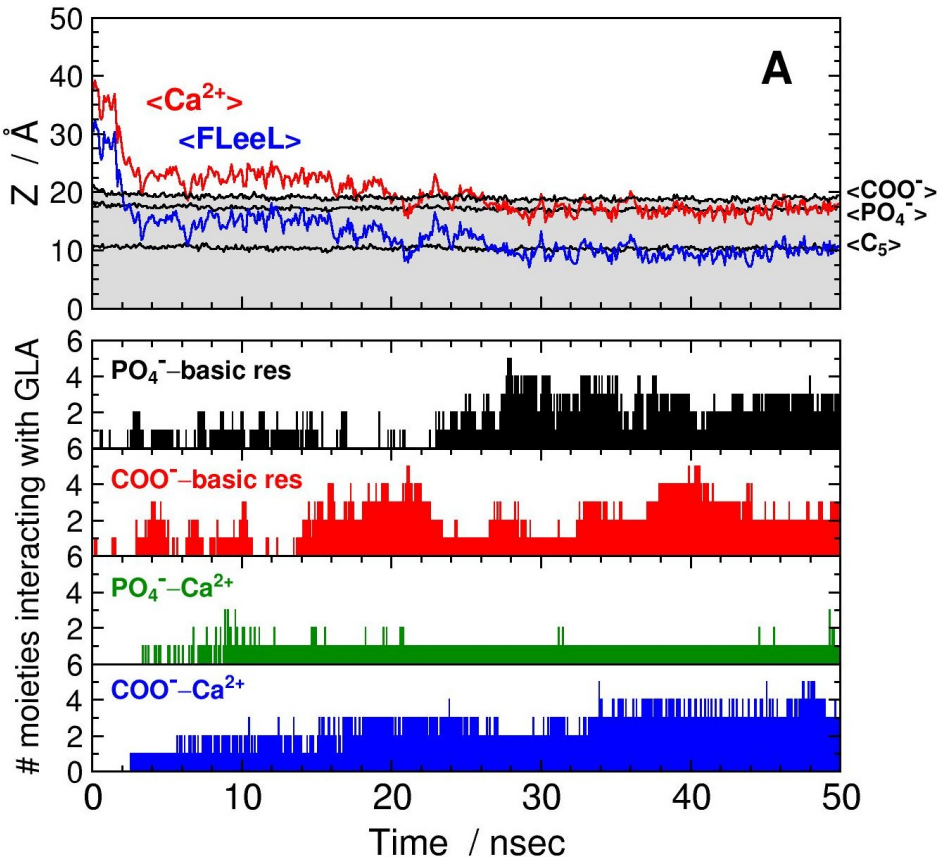

	Ca^{2+}-7	Ca^{2+}-8	Ca^{2+}-6	Ca^{2+}-5	Ca^{2+}-4	Ca^{2+}-3	Ca^{2+}-9	Total
# PO_4^-	0.00 (0.00)	0.00 (0.00)	0.00 (0.00)	0.00 (0.00)	0.00 (0.00)	0.44 (0.50)	0.00 (0.00)	0.44 (0.50)
# COO^-	0.86 (0.39)	1.08 (0.27)	0.00 (0.00)	0.00 (0.00)	0.00 (0.00)	0.00 (0.00)	1.44 (0.50)	3.38 (0.69)

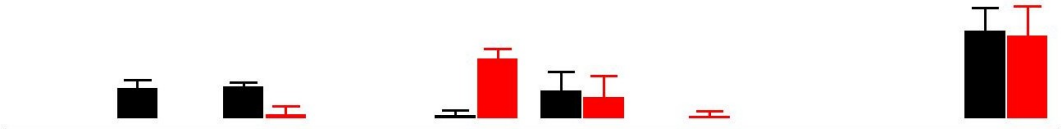

	R9	R15	K18	R28	K32	R36	K38	Total
# PO_4^-	0.91 (0.29)	0.98 (0.14)	0.00 (0.00)	0.04 (0.20)	0.84 (0.64)	0.00 (0.00)	0.00 (0.00)	2.77 (0.75)
# COO^-	0.00 (0.00)	0.08 (0.27)	0.00 (0.00)	1.88 (0.32)	0.62 (0.72)	0.03 (0.17)	0.00 (0.00)	2.61 (0.97)

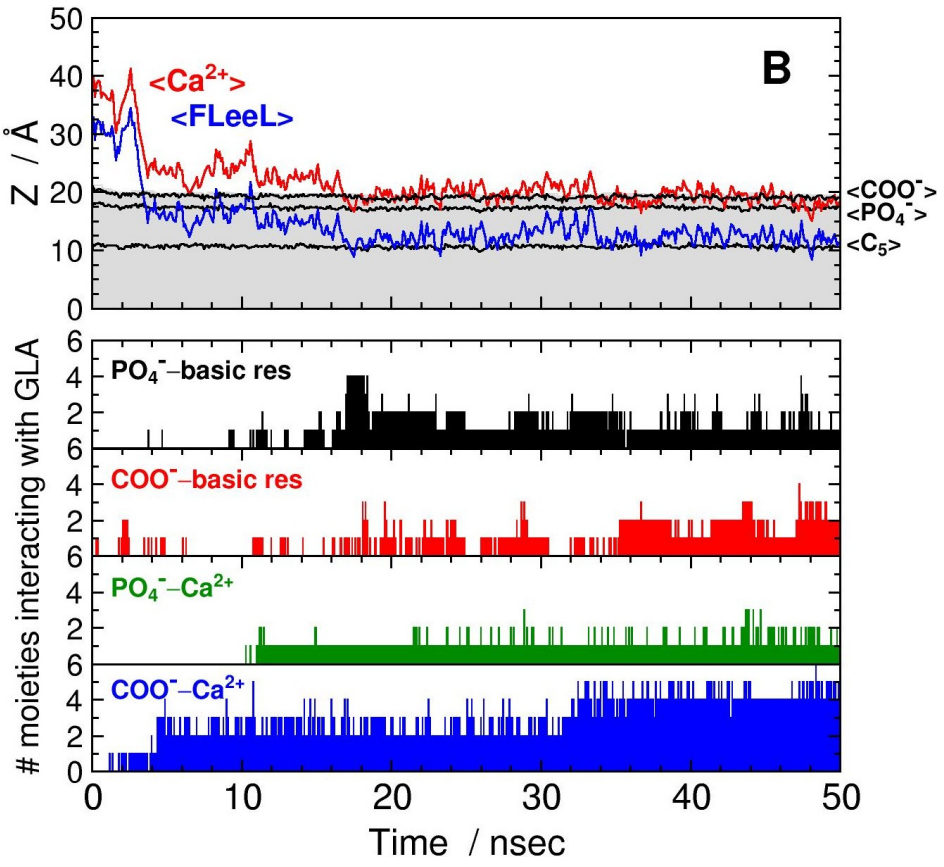

	Ca^{2+}-7	Ca^{2+}-8	Ca^{2+}-6	Ca^{2+}-5	Ca^{2+}-4	Ca^{2+}-3	Ca^{2+}-9	Total
# PO_4^-	0.00 (0.00)	0.25 (0.44)	0.00 (0.00)	0.00 (0.00)	0.00 (0.00)	0.03 (0.18)	1.02 (0.12)	1.31 (0.51)
# COO^-	1.18 (0.46)	1.02 (0.14)	0.00 (0.00)	0.00 (0.00)	0.00 (0.00)	0.43 (0.52)	0.62 (0.49)	3.25 (1.13)

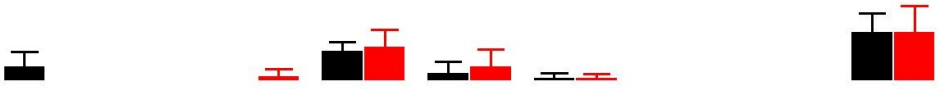

	R9	R15	K18	R28	K32	R36	K38	Total
# PO_4^-	0.39 (0.49)	0.00 (0.00)	0.00 (0.00)	0.90 (0.31)	0.18 (0.40)	0.03 (0.17)	0.00 (0.00)	1.50 (0.63)
# COO^-	0.00 (0.00)	0.00 (0.00)	0.07 (0.26)	1.01 (0.60)	0.40 (0.56)	0.02 (0.16)	0.00 (0.00)	1.50 (0.88)

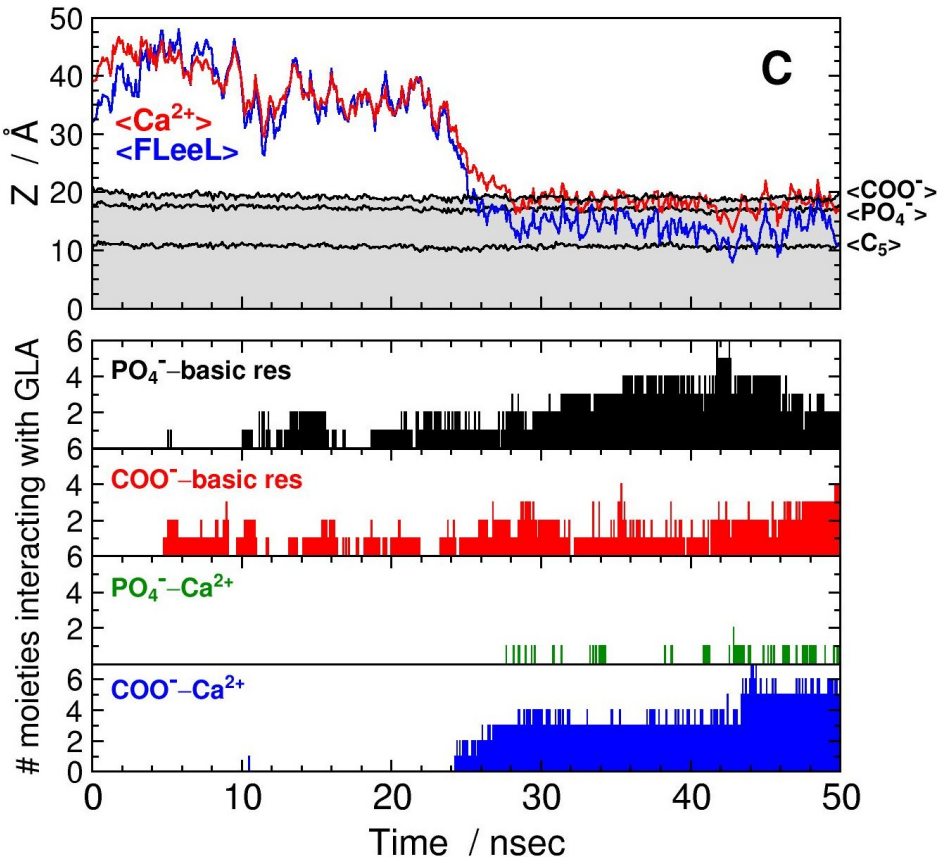

	Ca^{2+}-7	Ca^{2+}-8	Ca^{2+}-6	Ca^{2+}-5	Ca^{2+}-4	Ca^{2+}-3	Ca^{2+}-9	Total
# PO_4^-	0.00 (0.07)	0.16 (0.36)	0.00 (0.00)	0.00 (0.00)	0.00 (0.00)	0.00 (0.00)	0.11 (0.31)	0.27 (0.46)
# COO^-	1.31 (0.50)	0.38 (0.48)	0.00 (0.00)	0.00 (0.00)	0.00 (0.00)	1.00 (0.00)	1.32 (0.50)	4.01 (1.12)

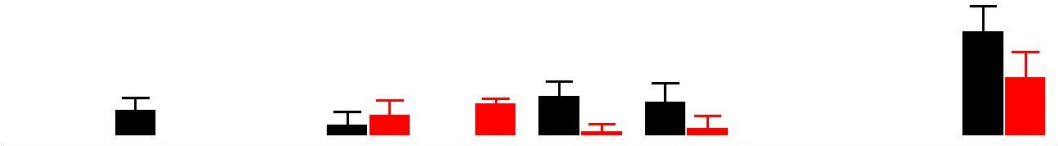

	R9	R15	K18	R28	K32	R36	K38	Total
# PO_4^-	0.77 (0.42)	0.00 (0.00)	0.29 (0.45)	0.00 (0.00)	1.22 (0.49)	1.01 (0.65)	0.00 (0.00)	3.29 (0.86)
# COO^-	0.00 (0.00)	0.00 (0.00)	0.60 (0.51)	0.96 (0.20)	0.07 (0.26)	0.18 (0.42)	0.00 (0.00)	1.81 (0.84)